Plastic Flow Modelling of a Hot-Rolling Manufacturing Procedure

Ben Hicks

Rolls-Royce plc

***Abstract**: During the qualification of a manufacturing technique, radiographic inspection revealed porosity in and around a weld. It was hypothesised that the cause of this porosity was associated with a previous manufacturing hot rolling procedure rather than an issue associated with the welding technique itself.*

A non-linear 2D representation of the component and manufacturing technique was modelled using Abaqus/Explicit to investigate the plastic flow of the material during the hot rolling procedure. This is a two stage rolling operation which plastically deforms the component at high temperature by passing current through an electrode wheel. A flange is formed by squeezing the material between two dies and, subsequently, the model included a number of contact definitions, high temperature and high strain rate dependent deformation and also utilised mass scaling to reduce the analysis runtime. Sensitivity to variation of a number of the manufacturing parameters was explored.

The analysis demonstrated a mechanistic root cause of the initial porosity found during the radiography and this was substantiated by good correlation with a number of controlled manufacturing experiments. The sensitivity analysis helped to identify the key parameters to control during the hot rolling procedure. Further to this, the assessment improved the understanding of the procedure and helped to identify improvements for Non-Destructive Examination (NDE) by bounding the potential extent of the concern.

***Keywords**: Upsetting, Forming, Hot-Rolling, Mechanistic Modelling, Mass Scaling, Viscoelasticity, Plasticity, Springback.*

1. Introduction

1.1 Background of the problem

Radiographic inspection of a welding test piece, carried out as part of welding qualification, detected an unusually large amount of porosity around a weld.

The region of concern was sectioned (through grinding and etching) and a defect was revealed in the flange region where porosity had been detected. The morphology of the defect at its greatest extent whilst sectioning is detailed in Figure 1 and this reveals a characteristically cruciform shaped void within the porosity.

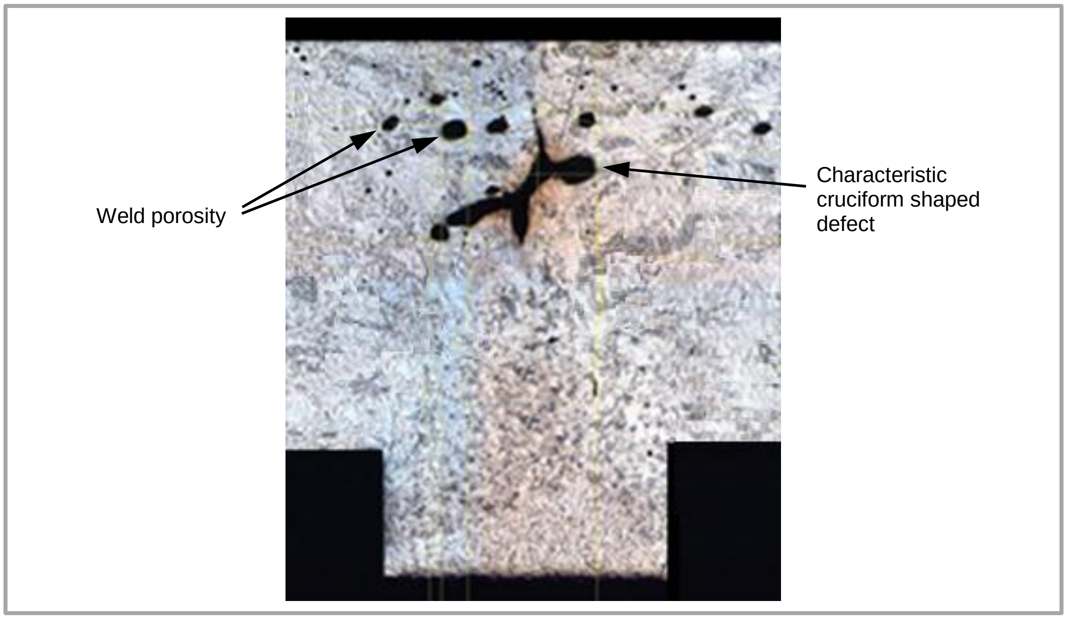

Figure 1 Sectioned weld qualification component illustrating weld porosity

1.2 Hypothesised cause

Based on the background of component manufacture, it was hypothesised that the cause of this porosity was associated with a previous manufacturing hot rolling procedure rather than an issue associated with the welding technique itself. The hot rolling technique is used to produce the flange on the end of the component during one of its intermediate manufacturing processes. This process forms the flange by plastically deforming the material at the edge of a plate into a forming die. It was hypothesised that if a linear defect existed in the plate then this may open as the plate is deformed to develop a feature similar to that observed in the sectioned component (Figure 1).

1.3 Hot-rolling procedure that creates the component flange

Force is applied by a rolling wheel electrode through which, at the same time, a high current is passed between the die and wheel causing resistive heating. The current generates high localised temperatures in the region where the material deforms whilst water cooling of the clamped region of the component is used to prevent deformation in undesired locations.

To verify whether or not this weld defect was due to the hot rolling procedure, Abaqus/Explicit was used to attempt to model the procedure and to establish whether the characteristic, cruciform, nature of the original defect could be reproduced using modelling software.

The hot-rolling process upsets component material protruding above the dies through two distinct passes of the rolling wheel. Each pass increases in depth which increases the quantity of material squeezed between the dies. The hot-rolling procedure is illustrated in Figure 2.

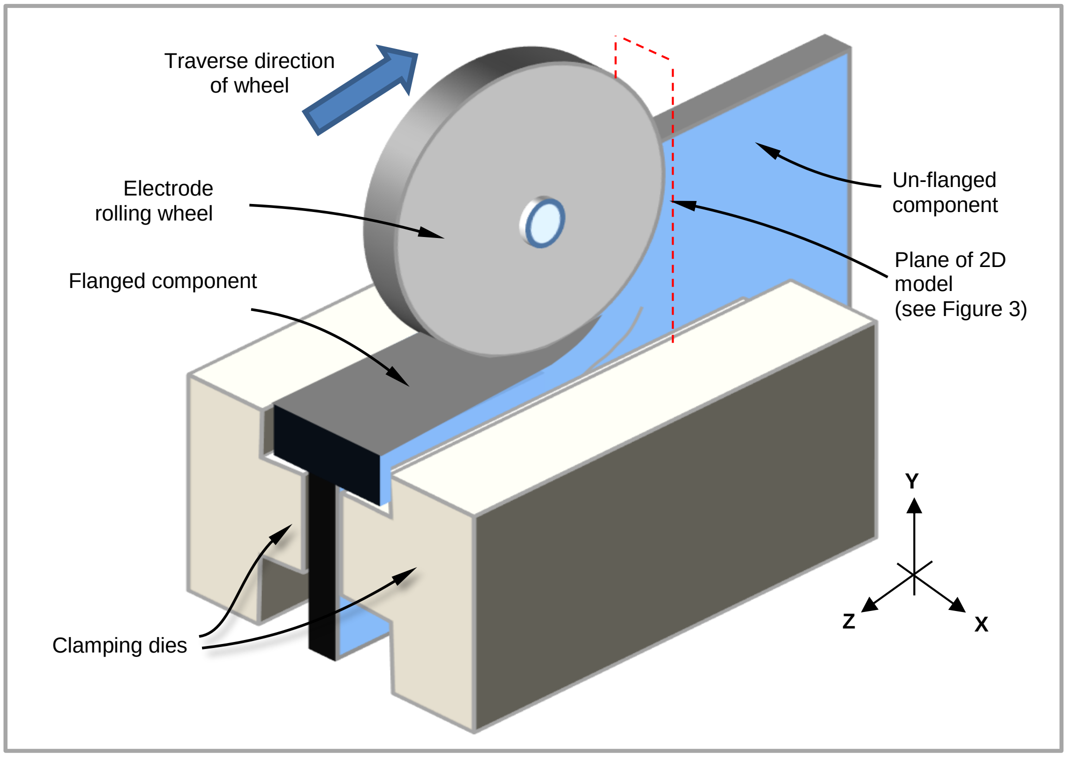

Figure 2 Illustration of flanging (hot-rolling) procedure

2. Process Modelling Setup

2.1 Model Setup

Initial assessments considered a simplistic 2D representation of the upsetting process using Abaqus/Explicit. Since the process involves large plastic deformation of the material, it is highly non-linear by nature. At the time of analysis, a number of manufacturing parameters were also unknown and this included the load in the wheel.

The model was created with separate components for each piece of tooling including the electrode wheel and each of the two halves of the die which clamp and form the component. The wheel was modelled as a single, rigid body and subsequently was only represented as a single contact surface onto the deformable component. The dies were created as analytically rigid objects but dimensions were oversized due, primarily, to convergence issues associated with the numerous contact constraints that were imposed on the model.

The edge of the component was created as a 2D planar deformable object. It should be noted that only the outer edge of the component is modelled since initial sensitivity analysis showed that material below the clamped region was unaffected by the hot-rolling process. The model is restrained in the y-direction at the base of the modelled region as indicated in Figure 3.

2.2 Analysis Steps

Due to the non-linearity of the model and the uncertainty of the load in the wheel and the clamps, the analysis was set up to be displacement driven, rather than load driven as in the manufacturing process, as this helps with solution convergence and additionally reduces solver time.

There are two key displacements in the process that are represented in the model as described below and represented in Figure 3.

Die Movement (Clamping of Component)

Representing the initial step of the process, a clamping force is created in the model by introducing a small displacement to each of the rigid body dies. The dies then maintain their position and a relatively constant clamping pressure throughout the remainder of the assessment. Sensitivity to the clamping force is discussed later.

Wheel Movement

Once the clamping process has been completed, the wheel is given a displacement to bring it into contact with the top of the plate. In initial models the wheel movement was applied at a constant rate. However, to further account for strain rate in later models, the rate of deformation was more accurately modelled by generating a sinusoidal profile to emulate the magnitude of wheel displacement in the plane of the model (ie the wheel surface moving vertically downwards as orientated in Figure 3).

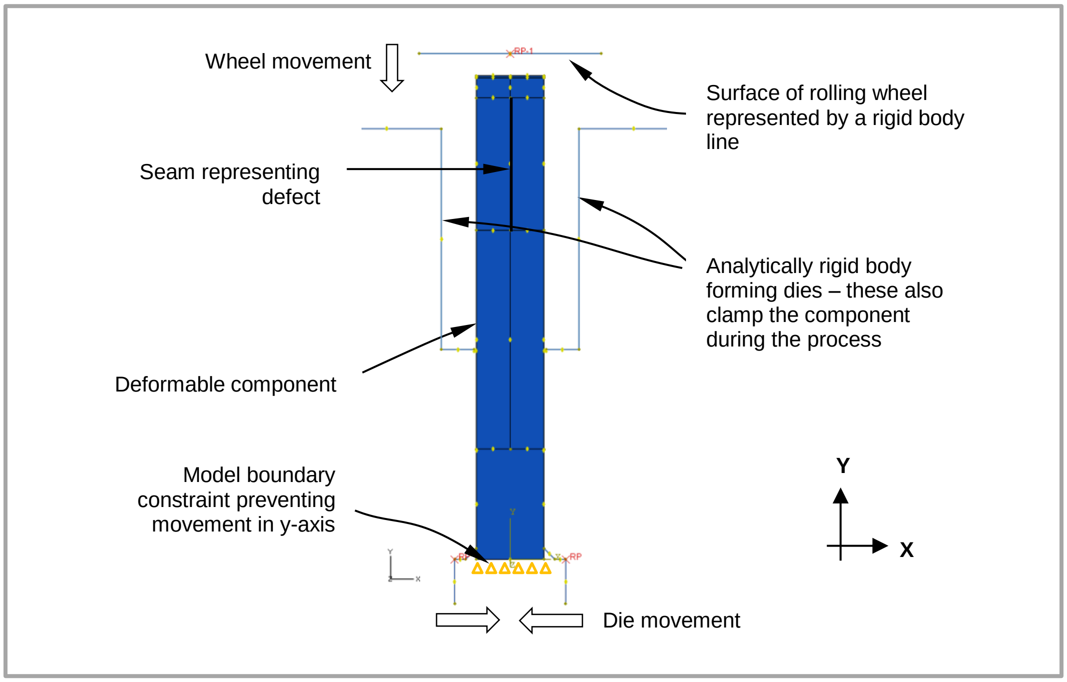

Figure 3 Components of the Abaqus/Explicit 2D hot-rolling model

The profile is generated as a function of the wheel diameter, the depth of pass of the rolling process and traverse speed of the wheel. The in-plane rate of deformation is another non-linear aspect of the analysis as shown and derived in Figure 4.

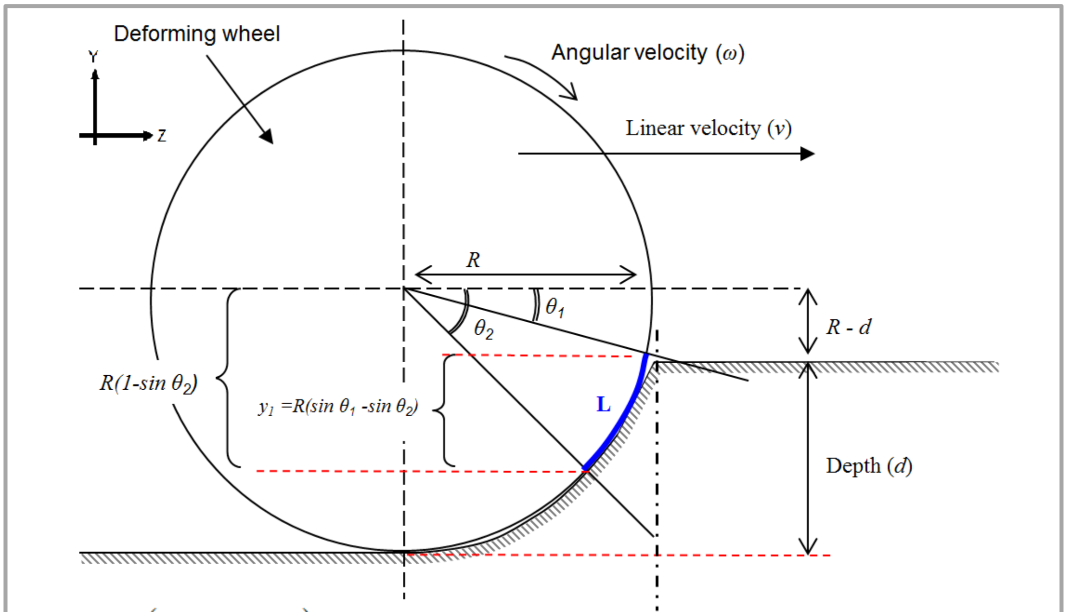

$$y_1 = R(1 - \sin \omega t) - d$$

Where: y_1 is the in-plane deformation

Figure 4 Derivation of the rate of deformation of the material in the X-Y plane

As the rolling process completes, the wheel is lifted from the surface of the model and this allows for a degree of relaxation (due to elastic springback) of the component. This occurs twice during the operation due to the two depths of rolling and each relaxation mimics the wheel lifting as it completes the staged pass.

2.3 Control Model

The initial process modelling aimed to produce a flanged component representative of a typically manufactured flange. This initial assessment was compared against another analysis package and with the manufacturing drawings to ensure that the deformed material was within specification. Each showed good correlation.

2.4 Hypothesised cause of weld porosity (defect)

The model was then developed to examine potential behaviour of linear defects in the material. These were replicated by introducing a seam into the Abaqus model (as labelled on Figures 3 and 5). The seam creates two disconnected nodes which overlap each other at each segment of the mesh along a line (ie each of the overlapping nodes along the seam have the same co-ordinates). Since the nodes are not connected, they behave as a linear defect within the component material.

2.5 Modelling contact

The model was set up with a number of contact definitions as illustrated in Figure 5. These include interaction with the dies, the surface of the wheel, the surfaces of the seam itself and the various instances of self-contact on each surface. Abaqus 6.8-3 was used for these assessments and, subsequently, although it would have been preferable to use general contact, it was not available at the time the models were constructed.

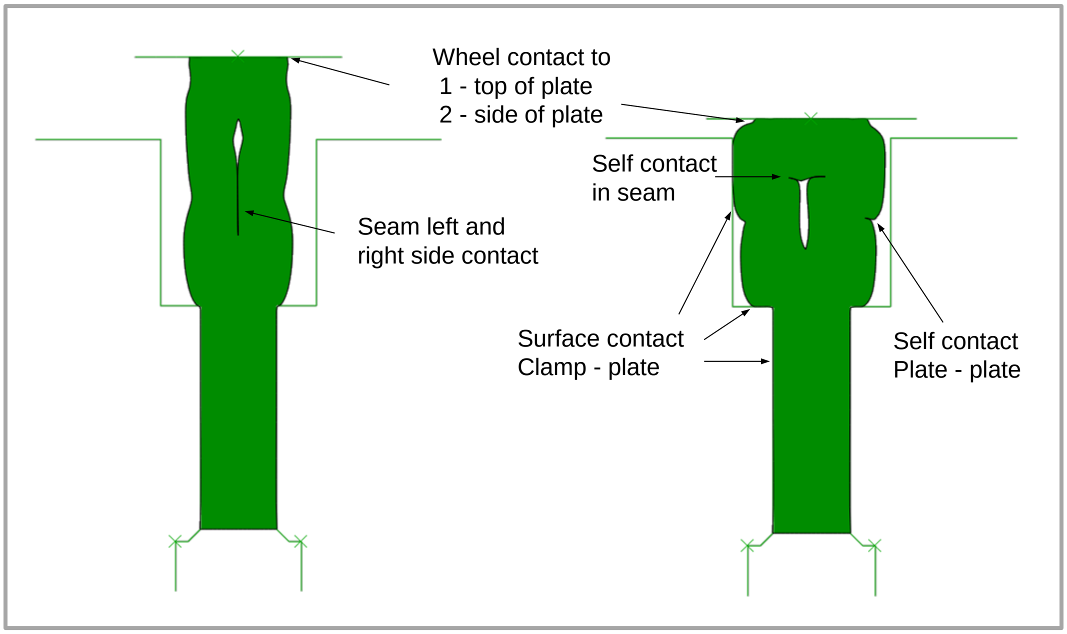

Figure 5 Contact definitions within Abaqus model as it deforms

The behaviour of the defect during the deformation process was examined in response to varying model parameters, such as changing material properties, and by varying the length and location of the seam. The model was also set up to allow asymmetric effects, such as buckling, to be examined.

3. Mechanism for formation of 'cruciform' defects

The results from the assessment with the seam demonstrated a mechanism for transforming a linear defect into a cruciform shaped void within a formed flange. The cruciform shape is generated due to bowing of the material surrounding the linear defect. As the bowed material contacts the sides of the die, the outer edges of the defect are restricted from growing thus limiting the extent of the horizontal component of the cruciform. Compression of the material from above eventually causes material to compress around the void to close the defect and leave the characteristic 'cruciform' shape. This process is illustrated in Figure 6.

Once the mechanism was established, it was identified that the model may be able to help bound the locations where a defect may deform to within the flange. The flange is also subjected to a number of loads throughout its lifetime and therefore, bounding the defect into a smaller size and limiting the location of its whereabouts helps to reduce the potential for crack growth, increase the resilience to fatigue and ultimately increases the lifetime of the component.

Bounding the location of the defect not only helps aid the argument for the structural integrity of the component but also establishes where Non-Destructive Examination (NDE) can be focussed to ensure there are no defects in a formed flange.

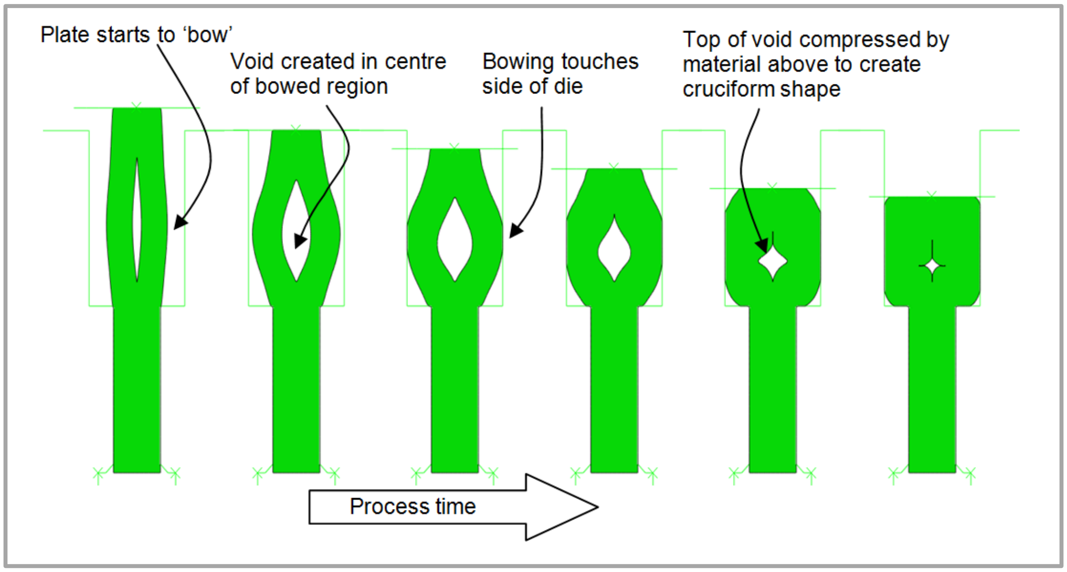

Figure 6 Mechanism for how linear defects can form cruciform voids

3.1 Sensitivity Analysis Requirement

Whilst the model demonstrated the mechanism for forming cruciform defects, it only showed a flat cruciform that does not bear much resemblance to the original defect (Figure 1). There are, however, a number of parameters that feed into the modelling that had not been explored at this stage. Analysis was carried out through a number of sensitivity analyses to establish whether or not the original defect could be recreated and to seek to bound the extent of defect formation.

To enable a thorough investigation on each influencing parameter, a large number of runs needed to be completed. Since the analysis is non-linear and had a number of contact calculations to solve, each assessment had a relatively large runtime and a number of techniques were investigated to help speed up the process. The techniques examined primarily included mesh optimisation and mass scaling. As part of this process, adaptive meshing was also considered due to the high deformation of the mesh especially around the defect.

3.2 Mass Scaling

Of the aspects considered, 'mass scaling' was shown to be highly beneficial in speeding up the analysis process. While the techniques reduce the accuracy of the solutions, a sensitivity analysis was used to determine the optimum quantity of scaling verses quality of result.

Although an in-depth analysis on mass scaling could have been completed, the uncertainties within operating parameters of the hot-rolling procedures indicate that there will always be a degree of uncertainty within the accuracy of any converged solution. Subsequently, using a standard model, which includes a defect, solutions were compared for varying levels of mass scaling and the degree of similarity between the distortions and displacements of the original solution, Figure 7, were weighed up against the time saved in resolving the problem, Figure 8.

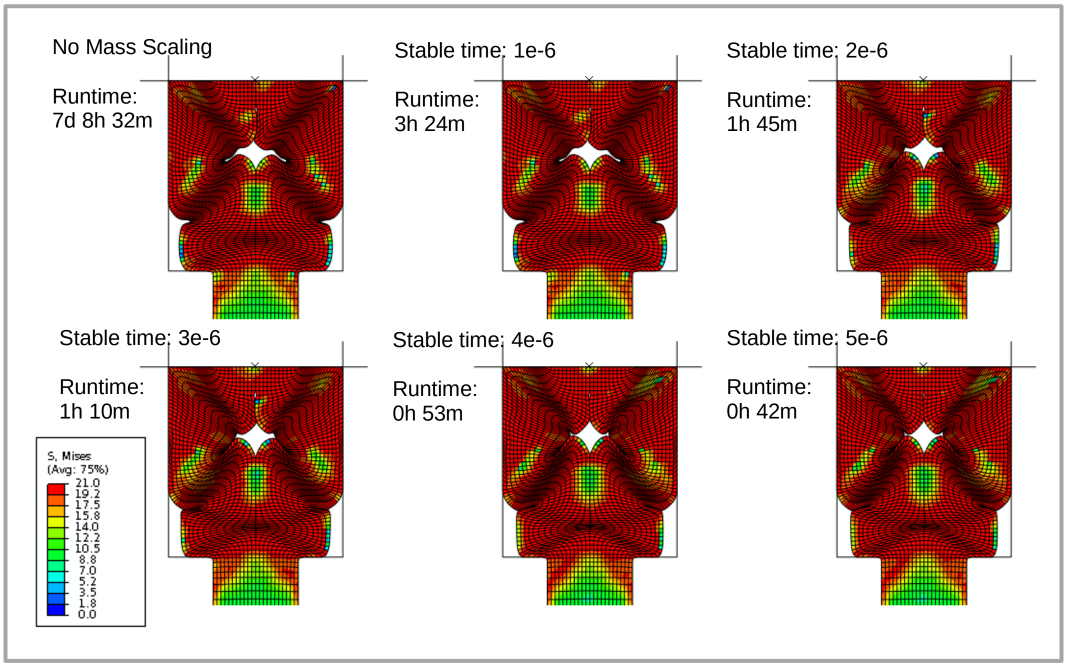

Figure 7 Illustration of the effect of mass-scaling on the analysis solution

Once the mesh was optimised and a suitable level of mass scaling was applied, a number of sensitivity analyses were undertaken. Initially these focused on some of the operating parameters of the hot-rolling procedures including assessment of the clamping force, angular variation between the component and wheel, sensitivity to the size and location of the defect and, finally, assessment of the component temperatures along with associated changes in material strain rate.

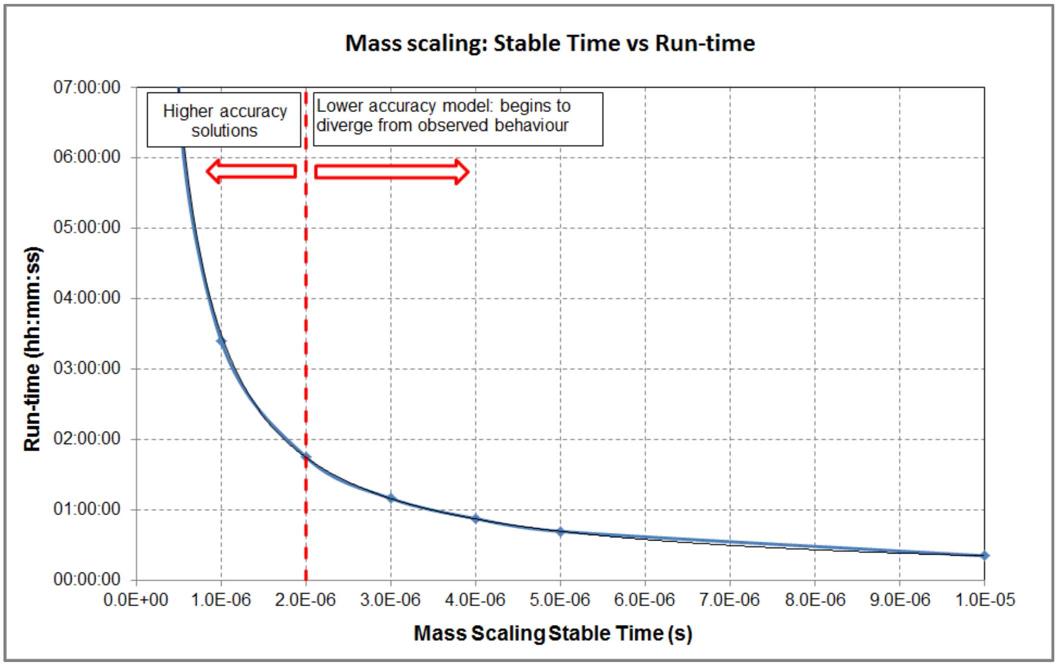

Figure 8 Illustration of the effect of mass-scaling on the analysis runtime

3.3 Limitations of Modelling

Uncertainties in the setup of the model pose significant issues with regard to its validation and verification. Consequently, when analysing the results, the following assumptions were considered:

- No 3D effects were examined, subsequently, the forces out of plane of the model were not examined and, additionally, the defect is assumed to run the length of the rolled component (ie out of plane). This assumption could affect the depth, size and location of where a defect may form.
- Material data was interpolated to obtain values at high temperatures and strain rates. Stress-strain data were defined for various equivalent plastic strains at a variety of temperatures using the *PLASTIC, RATE keyword and the materials were subsequently modelled using the default isotropic hardening parameter. However, material properties are not accurately measured at these temperatures, some of the applied data relies on modelled test data which introduces further imprecision. To further compound the problem, the temperature distribution during the process is also not accurately known and this, in itself, defines which of these material properties are used. The behaviour of the defect was shown to be sensitive to this parameter.

- In reality, a small amount of flashing can occur between the surface of the dies and the rolling wheel. The model used oversized dies to prevent flashing as the phenomena causes problems with convergence due to contact issues which result in failure to complete the analysis.
- The actual wheel displacement is governed by force control. However, given other uncertainties in the model, this cannot be accurately deduced and so an assumed displacement is the most suitable alternative.
- It is assumed that, during the deformation process, the modelled defect cannot open up any further (ie crack propagation is not accounted for). Additionally, since the process is at high temperature and pressure, there is also potential for the metal to re-bond and 'heal'. Neither of these aspects are accounted for within the modelling.
- Both the dies and the rolling wheel are assumed to be rigid bodies.

4. Manufacturing Trials

Whilst the Abaqus modelling was underway, some manufacturing trials were carried out with the intent of replicating the cruciform defect by artificially creating linear defects in the material before upsetting it using the hot-rolling machine. This was done independently of the modelling and was used to provide confirmation of the defect formation mechanism and to also provide some degree of validation for the analytical modelling method. Destructive and non-destructive techniques were used to determine the size and location of defects in the upset flange.

The upsetting trials were undertaken looking at varying the locations and sizes of defects. This essentially represents changes in the depth and length of the modelled seam in the Abaqus models. Additional control trials were also constructed to ensure that observed effects were not due to another aspect of the upsetting process.

Although defects were created at similar sizes to the modelled defects, inaccuracy in the location of the defect could help account for discrepancies between trial and model data. Figure 9 shows some of the sectioned specimens from the trials.

4.1 Images of Sectioned Trial Specimens

Each defect appears to have significant gape, however, this is largely a surface effect due to the etching process used in metallurgical preparation of the specimens. Etching rounds off the sharp edges of voids making them appear wider than they actually are. Furthermore, the images have been obtained using a reflected light microscope. This exaggerates the volume of a feature with rounded edges because light from the edges is not reflected directly back through the microscope.

Without careful examination, this gives the impression of a void which has the same cross-sectional area through its whole depth as it does at the surface. Examination of defects in an unetched condition at significantly higher magnification using a scanning electron microscope confirms the lack of a volumetric component.

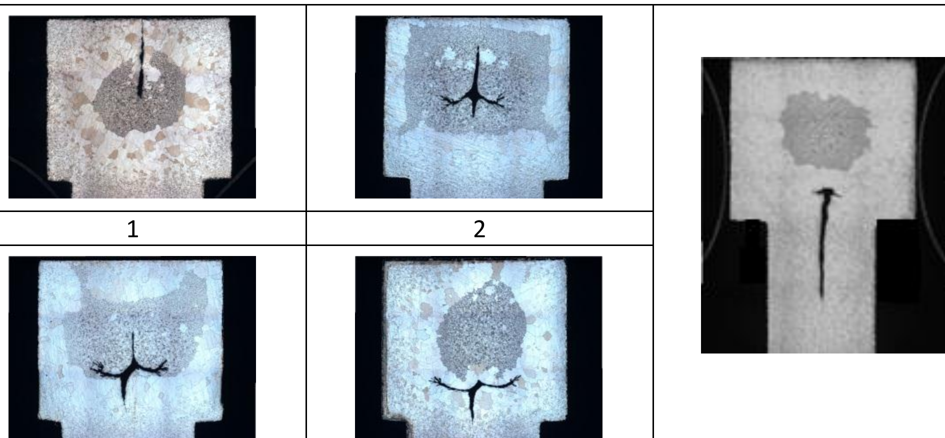

The increasing number of the images represent increased depth of linear defect location. In each case, the defect size is the same for each sectioned image.

Figure 9 Sectioned images from manufacturing trials

5. Modelling and Trials Comparison

5.1 Model verification - comparison of model and trial results

Model predictions were compared with the equivalent trial results to show varying levels of agreement. Figure 10 illustrates some of the key successes which were identified. However, some inconsistencies between the results were also found and these can be attributed to the large number of variables and uncertainties in the model – most notably coming from interpolated materials data and unknown temperature distribution – both of which can have a significant impact on formation of the flange.

5.2 Non-sensitive process parameters

The force applied to clamp the component was unknown and so a rough estimate, based on a small displacement, was applied. Sensitivity analysis of the clamping force was then carried out by varying this displacement. Overall this force was shown to be a non-sensitive parameter in influencing the formation of the defect.

Variation on the width of each side of the die was also investigated and the worst-case scenario was found to be applicable for larger width dies as this resulted in larger volumetric defects (ie larger horizontal components). For other sensitivity analyses, the die width was set at the upper tolerance to get a worst case scenario for the volumetric size. A slight change in the defect location could also be observed as the die width was altered, however, this was deemed insubstantial especially considering the variability applicable from other influencing factors.

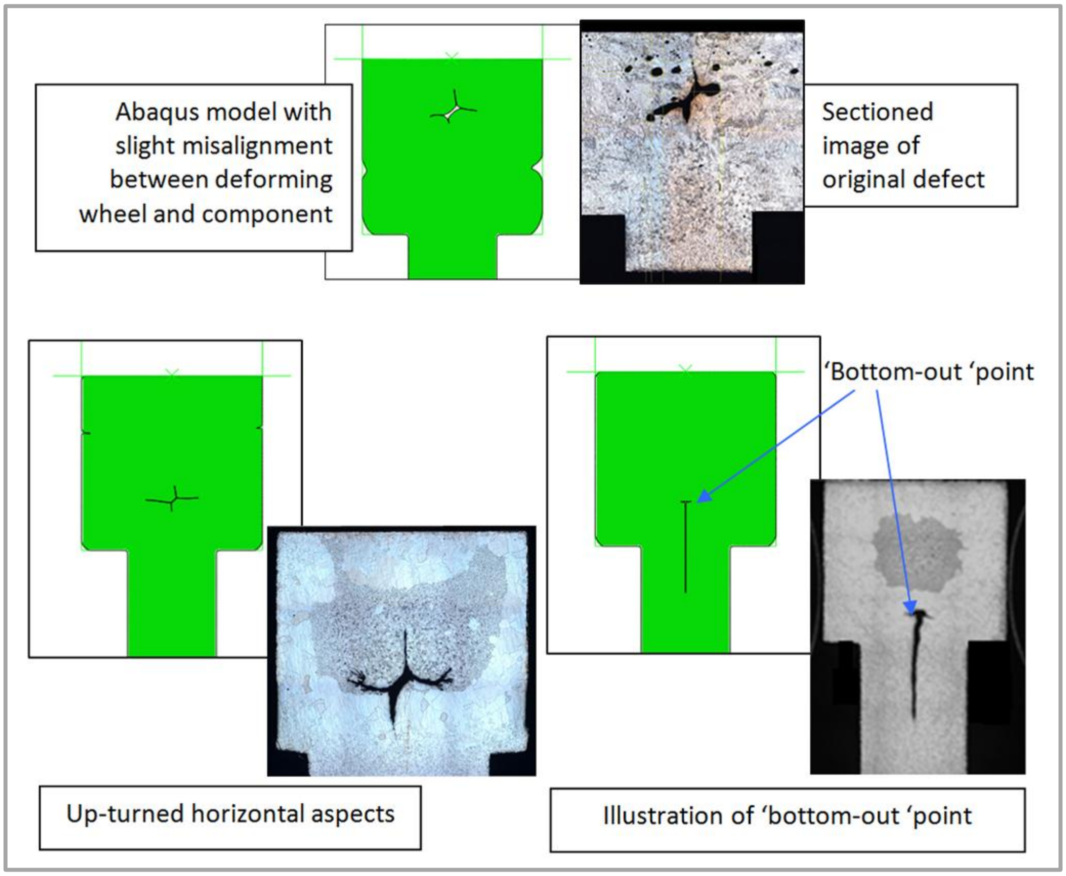

Figure 10 Examples showing correlation between model and trial predictions

5.3 Influential model parameters

Angular difference between wheel and plate

An angled contact between the plate and rolling wheel could occur systematically from a skewed spindle on the wheel or alternatively, and more likely, from a slight manufacturing deviation off 'square' between the top and sides of the component. Observations from the analysis show that the angle at which the horizontal aspects of the cruciform can form is highly sensitive to this angle between the top of the undeformed plate and the wheel. Depending on other modelling aspects, an angle as small as 0.1° can rotate a cruciform defect as much as that seen in the originally sectioned flange. This sensitivity clearly explains why the original defect appears to be angular by nature.

Variation in Defect Location and Size

Models were created with defects of varying sizes starting at staggered depths along the centre line. Overall, results showed a number of scenarios where volumetric defects (those that have horizontal aspects and therefore form a cruciform) could occur along the centre line. Varying this location and size alters where the ‘bowing’ mechanism begins and, in turn, controls the depth at which a defect may occur in the flanged specimen.

For small lengths of linear defect, the flanged component produces little to no horizontal aspect to the defect as the material is incapable of ‘bowing’ to a significant enough extent. A larger linear defect determines whether or not the characteristic ‘cruciform’ shape can start to occur.

Final defects may vary in width depending on the depth of the original linear defect. However, width was shown to be largely controlled by the contact with the outside of the dies and, therefore, large linear defects will transform into defects of limited maximum width regardless of their size within the flange.

Temperature Distribution

A significant change to the formation and shape of volumetric defects can be observed if the process temperature is altered slightly. The temperature profile through the component is largely unknown and could have a range extending over 200°C in a small area due to the localisation of resistive heating. Since the presence of a defect can also change the component temperature profile, a simple model with a representation of this parameter can explain many of the discrepancies between predictions and the manufacturing trials data.

5.4 Summary of modelling

Overall the process modelling predicts how a linear defect near to the edge of the component can behave during the flanging process. It suggests that a significant number of variables can interact to alter the size, shape and formation of defects created through the flanging process. Currently, the parameters affecting these interactions are not quantifiable and, in some cases, may, in themselves, alter depending on the size and presence of a defect. For example, changes in the temperature profile across the component can significantly affect the way the material behaves under deformation. However, the temperature distribution in the component can, in itself, be dependent on the presence and location of any potential defects.

The test piece images all show an area of material, in roughly the middle of the flange, which has a grain structure different from the surrounding material (see images in Figure 9). This non-homogeneity is caused by the heat input during flanging and is eliminated during post flanging processes (hence the apparent lack of grain structure presented in Figure 1). It can be noted in the sectioned trial images that the grain structure areas differ for different locations of defect. This difference supports the argument that the defect itself affects the heat dissipation through the component during the flanging operation.

6. Key Characteristics Obtained from Trials and Models

6.1 Cruciform depth

When comparing model and trial data, it appears that the final location of the vertical aspect of the defect can be predicted fairly accurately. However, there is some discrepancy with the predictions of the location of the horizontal component. The disparity has been shown, through sensitivity analysis, to be primarily related to the temperature distribution and, consequently, the material properties in the model.

6.2 Bottom-out point and horizontal ligament

Importantly, the results exhibit important characteristics where the model features defects that extend to a substantial depth below the surface. These defects reach a depth, referred to as the bottom-out point (as shown in Figure 10), where there is no mechanism allowing them to bow and form horizontal aspects to the defect. In the mechanism that transforms a linear defect into a cruciform shaped void, it is judged that the defect would be likely to open up only when the material is subject to high tensile stress, such as that occurring when the component undergoes the large deformation seen in the flanging operation. Material below the bottom-out point sees very little deformation as it is under compressive lateral stress, which prevents outward bowing of the material. The presence of a continuous defect below the bottom-out point does not bow out owing to insufficient strain.

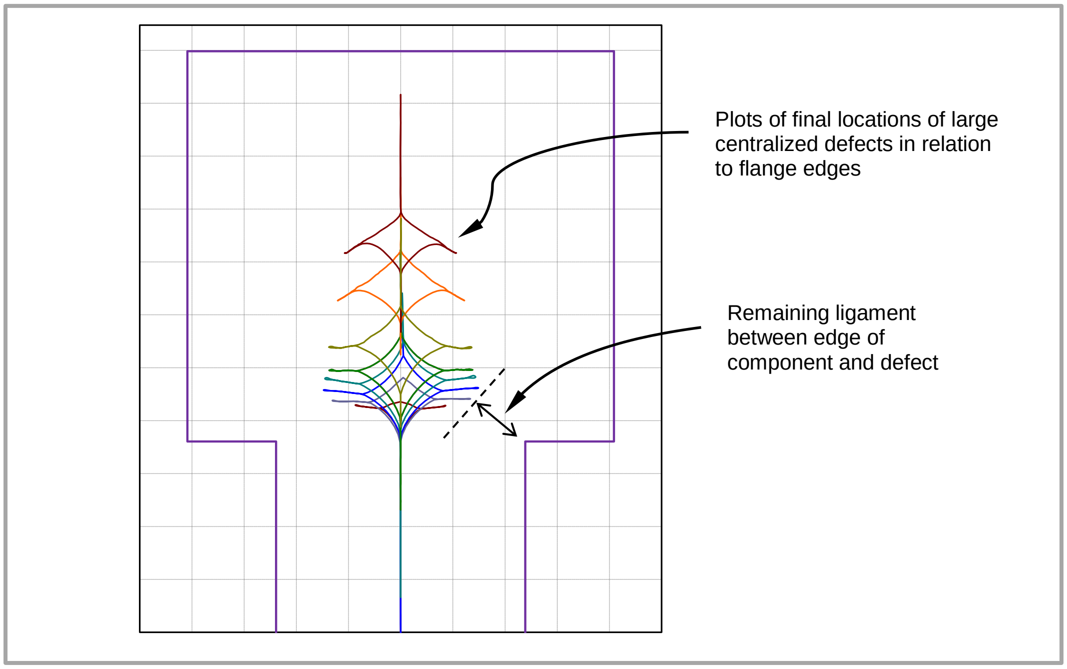

Figure 11 Scope and location of modelled defects and minimum ligament

Figure 11 identifies the resultant formation of defects from the staggered depths of centralised large linear defects. The width of the horizontal component increases slightly until the defect approaches the bottom-out point where the width reduces significantly and, subsequently, results in a larger remaining ligament to the edge of the component.

It is therefore judged that a linear defect within the material below the bottom-out point will not break open to form horizontal components to a defect. Whilst the model over-predicts the location of the bottom-out point, the actual value can be measured from the trials sections. The difference is likely due to three main factors: neglecting 3D effects, the inaccuracy of the temperature distribution and the variability in material properties. Evidence of these effects has been demonstrated through the various sensitivity analyses.

The importance of this result is that it implies that in all instances there will be sufficient ligament remaining between horizontal aspects of any defect and the base of the flange. This will prevent full fracture of the component in this area when subjected to an anticipated worst case loading.

6.3 Conclusions

Trials and modelling confirm the mechanism for formation, during upsetting, of a cruciform flange defect from an initial linear defect. Both trials and modelling predict a bottom out point for the horizontal aspects of this defect. The trials data has subsequently been used to establish a reliable figure and to feed into a failure analysis. Both trials and modelling also predict a maximum defect width and associated minimum ligament between the defect and the bottom edge of the formed flange.

An in-depth review of manufacturing processes and inspections, defect formation trials and analytical modelling of the mechanism that could cause the observed porosity in the welded region have successfully demonstrated that this porosity was generated through a pre-existing linear defect.

7. References

1. Abaqus Users Manual, Version 6.8-3, Dassault Systémes Simulation Corp., Providence, RI